# Triple Modification of Alginate Hydrogels by Fibrin Blending, Iron Nanoparticle Embedding, and Serum Protein-Coating Synergistically Promotes Strong Endothelialization

*Alena Richter,\* Yaya Li, Christoph Rehbock, Stephan Barcikowski, Axel Haverich, Mathias Wilhelmi, and Ulrike Böer*

**Stent therapy can reduce both morbidity and mortality of chronic coronary stenosis and acute myocardial infarction. However, delayed re-endothelialization, endothelial dysfunction, and chronic inflammation are still unsolved problems. Alginate hydrogels can be used as a coating for stent surfaces; however, complete and fast endothelialization cannot be achieved. In this study, alginate hydrogels are modified by fibrin blending, iron nanoparticle (Fe-NP) embedding, and serum protein coating (SPC) while surface properties and endothelialization capacity are monitored. Only a triple, synergetic modification of the alginate coating by simultaneous I) fibrin blending, II) Fe-NP addition complemented by III) SPC is found to significantly improve endothelial cell viability (live–dead-staining) and proliferation (WST-8 assay). These conditions yield formation of closed endothelial cell monolayers and an up to threefold increase (p < 0.01) in viability, while, interestingly, no effect is found when the modifications (I)–(III) are conducted individually. This synergetic effect is attributed to an accumulation of agglomerated Fe-NP and serum proteins along fibrin fibers, observed via laser scanning microscopy tracking nanoparticle scattering and tetramethylrhodamine (TRITC)-albumin fluorescence. These synergetic effects can pave the way toward a novel strategy for the modification of various hydrogel-based biomaterials and biomaterial coatings.**

## 1. Introduction

Coronary heart disease is the most common cause of death with 7.2 million people worldwide per year.[1] Among the different available therapies, stent therapy is able to reduce both the morbidity and mortality of coronary heart disease and its acute complication, the myocardial infarction. Therefore, stent therapy has become the primary therapy for acute ST-elevation myocardial infarction.[2] Nevertheless, in-stent-restenosis resulting from thrombo-embolic events, neointimal hyperplasia, or neoatherosclerosis is still the limiting factor of successful invasive stent therapy.[3,4] The underlying pathomechanism of these failures includes delayed re-endothelialization and endothelial dysfunction which are further aggravated by hypersensitivity reactions to synthetic polymers resulting in chronic inflammation.[1,5] Therefore, the development of a biocompatible stent device enhancing functional endothelialization is highly required. Biological polymers, especially, are attracting more and more interest. Among those are protein-based polymers like fibrin[6] or polysaccharide-based polymers like alginic acid.[7]

Alginate hydrogels have been suggested as biological stent-coatings since they have been characterized by high biocompatibility and a so-called "non-fouling" effect.[8] Due to the absence of any adhesive structures and high surface wettability, alginate

A. Richter, Prof. A. Haverich, Prof. M. Wilhelmi, Dr. U. Böer
Lower Saxony Centre for Biomedical Engineering
and Implant Research and Development (NIFE)
Hannover Medical School
30625 Hannover, Germany
E-mail: richter.alena2@mh-hannover.de

The ORCID identification number(s) for the author(s) of this article can be found under https://doi.org/10.1002/admi.202002015.

Y. Li, Dr. C. Rehbock, Prof. S. Barcikowski
Technical Chemistry I and Center for Nanointegration Duisburg-Essen (CENIDE)
University of Duisburg-Essen
Universitätsstr. 5–7, 45141 Essen, Germany

Prof. A. Haverich, Dr. U. Böer
Division for Cardiac-, Thoracic-, Transplantation- and Vascular Surgery
Hannover Medical School
30625 Hannover, Germany

Prof. M. Wilhelmi
Department for Vascular and Endovascular Surgery
St. Bernward Hospital
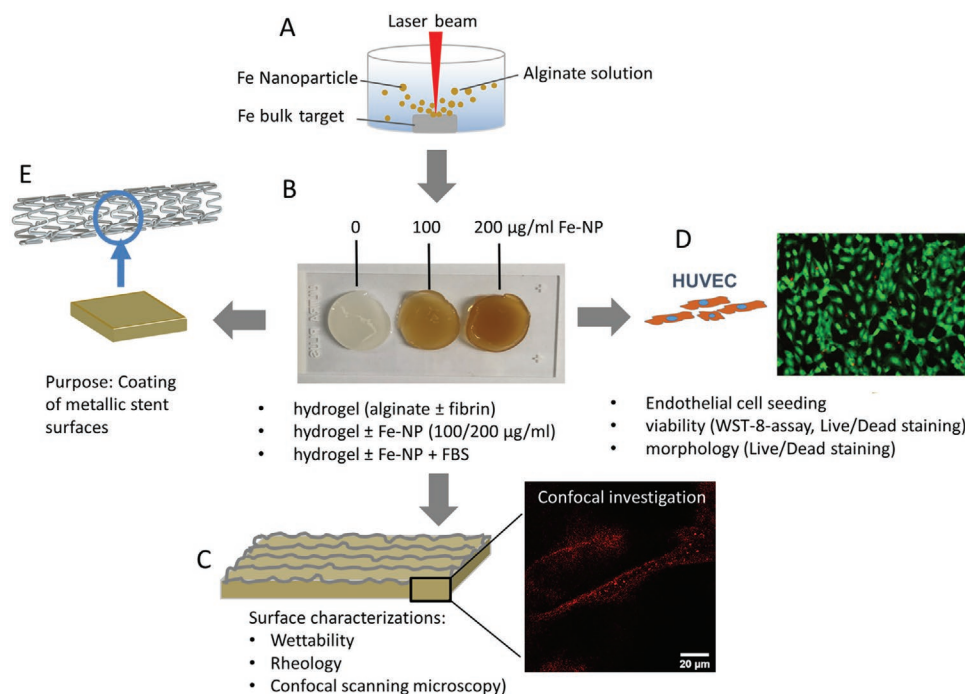Treibestr. 9, 31134 Hildesheim, Germany

**Figure 1.** Overview of the study performed. A) Iron nanoparticles manufactured by laser ablation in aqueous alginate solution were used to enrich B) alginate- and alginate-fibrin-hydrogels. C) Hydrogels were characterized for wettability, rheological properties and by confocal microscopy and D) seeded with endothelial cells with E) the purpose to coat metallic stent surfaces for better biocompatibility and antithrombotic properties. Fe = iron, NP = nanoparticle, FBS = fetal bovine serum, HUVEC = human umbilical cord endothelial cells.

gels do not support platelet and bacterial adhesion and thereby prevent in-stent-thrombosis[9] and the formation of biofilms.[10] However, the non-fouling effect also avoids beneficial protein adsorption and endothelial adhesion[11] thus compromising the antirestenotic properties of alginate-coated stents. For this reason, a modification of alginate hydrogels is highly desirable to enable the adhesion and proliferation of endothelial cells.

Metal ions incorporation recently has been shown to change alginate hydrogel properties in terms of mechanical strength[12] and to promote fibroblast proliferation by decreasing gel hydrophilicity which most likely improved protein adsorption.[13] In particular, ferric ions have been shown to support these effects. To avoid fast ion release into the entire medium and related potential toxicity, the embedding of metal nanoparticles as depots for ions can be a promising alternative. Iron nanoparticles (Fe-NPs) integrated into hydrogels have been reported as a suitable strategy to achieve improved bio response.[14,15] Moreover, the cellular compatibility of alginate gels was extended to endothelial cells by incorporation of Fe-NP leading to a sustained beneficial effect of ferric ions enhancing endothelial cell adhesion.[15] Previously, we have reported on the relationships between iron ion release and protein adsorption and found a strong synergy between the two even at very low Fe-NP mass loads.[16] It is well known that biomaterials come into immediate contact with serum proteins and form a protein layer, which gives an important identity to a stent.[17] Finally, blending with other polymers is an option to modify alginate hydrogels. Fibrin is a natural polymer with multiple cell adhesion sites[18] that recently has been used for stent coating.[6] Furthermore, the fibrin-alginate interpenetrating networks seemed to exhibit

well tunable mechanical and adhesive properties at varying fibrin concentrations.[19] Inspired by these results we triple-modified alginate gels with Fe-NPs, fibrin, and serum protein coatings (SPCs). Here, we were particularly interested in synergetic effects between the three types of modification and their impact on the physicochemical properties of alginate surface and the resulting cell behaviors.

Hence, in this study we provide an in-depth investigation of the cell response on the different hydrogel surfaces. First, the method of pulsed laser ablation in liquids[20] was utilized to embed Fe-NP into alginate gels using an established in situ method.[15,16] Afterward, the Fe-alginate composites were blended with fibrin and consecutively coated with serum proteins. These hydrogel surfaces were thoroughly characterized including an evaluation of their mechanical properties. Eventually, endothelial cells were seeded on the triple-modified hydrogel surfaces while viability and proliferation of the cells were monitored.

## 2. Experimental Section

**Figure 1** gives an overview of all methods used in this study and the workflow.

### 2.1. Fabrication of Iron Nanoparticles by Laser Ablation

A laser ablation method was used to prepare Fe-NP directly in 1.5% (w/v) alginic acid (Sigma Aldrich) aqueous solution. In detail, the laser beam was produced by a picosecond (<10 ps)

**ADVANCED
SCIENCE NEWS**

www.advancedsciencenews.com

**ADVANCED
MATERIALS
INTERFACES**

www.advmatinterfaces.de

Nd:YAG laser system (Atlantic, Ekspla, Vilnius, LT) at the wavelength of 1064 nm and a repetition rate of 100 kHz, which was focused via a 100 mm lens on the iron bulk metal plate target with a thickness of 0.25 mm (purity 99.99%, Sigma-Aldrich, Saint Louis, USA). The target was fixed in a Teflon batch chamber with a solution volume of 30 mL under stirring. The target was weighed before and after the laser ablation process on a balance (Precisa 300–9234/H PESA Waagen, Switzerland) to determine the ablated mass of Fe-NP in the solution and to determine iron concentrations and mass loads in the hydrogel. The obtained Fe particle size in the alginate gel was analyzed by transmission electron microscopy (TEM; Zeiss EM 910, 120 kV acceleration voltage) and the size distribution was plotted with Origin software.

### 2.2. Fabrication of Alginate Hydrogels

Alginic acid (1.33%; Sigma-Aldrich, Steinheim, Germany) enriched with laser-ablated Fe-NPs in two different concentrations, 102 and 204 µg mL$^{-1}$ (referred to as 100 and 200 µg mL$^{-1}$) was used for hydrogel fabrication (Figure 1B). Prior to polymerization, alginate solutions with or without Fe-NPs were autoclaved for 30 min. Cell culture tested low melting agarose (1.5% [w/v]) (Carl Roth GmbH + Co.KG, Karlsruhe, Germany) and CaCl$_2$ (2.5% [w/v]) were dissolved, autoclaved, and filled into 96-well-plates (75 µL) or 24-well-plates (500 µL) serving as a base-layer delivering the cross-linking Ca$^{2+}$ cations. The base-layer was allowed to polymerize for 30 min prior to the addition of alginate solution (75 µL in 96-well-plates; $n = 6$ for each group, 500 µL in 24-well-plates; $n = 2$ for each group). After 45 min of gelation the hydrogels were covered with ultrapure water until cell seeding.

For alginate-fibrin hydrogels, 5 or 10 mg mL$^{-1}$ fibrinogen ($n = 6$ each) and 0.5 I.U thrombin (CSL Behring GmbH, Marburg, Germany) per 10 mg fibrinogen were added to alginate solutions. Fibrinogen was isolated from human plasma obtained from donors after informed consent (Institute for Transfusion Medicine, Hannover Medical School) by cryo-precipitation as described previously.[21]

Alginate hydrogels were used either directly in cell culture experiments or stored prior to seeding to promote formation of degenerative pores. For this, hydrogels covered with ultrapure water were kept at 4 °C for 8 days.

For coating with serum proteins, hydrogels were covered with fetal bovine serum (FBS; 100 µL in 96-well-plates, 300 µL in 24-well-plates) for 3 h at 37 °C after gelation. Unbound proteins were removed by washing the hydrogels with ultrapure water. For visualization of protein coating, TRITC-coupled albumin (Thermo Fisher, Braunschweig, Germany) was diluted 1:500 with FBS and incubated on the gels as before. After washing twice with PBS the gels were analyzed with confocal laser scanning microscopy (LSM) (see below).

### 2.3. Hydrogel (Surface) Characterization: Wettability and Rheology

The wettability of biomaterials was evaluated by the captive bubble method to measure contact angle at the liquid-solid surface using the device OCA-15 (Dataphysics, Filderstadt, Germany) equipped with a video camera. The contact angles of air bubbles and water were measured with hydrogel films fixed on a glass substrate, facing downward in the water phase contained in a square transparent glass vessel. The air bubble was released from the J-shaped microsyringe needle beneath the glass substrate and attached to the biomaterial surface. The images were captured within 30 s and contact angles were calculated and recorded by the software SCA20-F provided by the company.

The relative stiffness of overall hydrogels was determined by performing oscillatory rheological measurements using the device Physica MCR 301 (Anton Paar, Ostfildern-Scharnhausen, Germany) at 20 °C. A 15 mm parallel plate was used and the normal force was set at 0.03 N. The strain sweep was in the range of 0.4–2% at an angular frequency of 0.5 rad s$^{-1}$. The elastic moduli ($E$) were determined from the storage modulus ($G'$) using the following equation:[22]

$$E = 2 \times G'(1 + \upsilon) \tag{1}$$

where $\upsilon$ = Poisson's ratio of 0.5 for hydrogels. The significance level between groups was performed with one-way ANOVA and $t$-test in Origin (Origin software, Originlab, Massachusetts, USA).

### 2.4. Surface Characterization of the Gels by Confocal Microscopy

The hydrogels prepared in 24-well-plates were cut into a thin layer placed on the glass slide and covered with a coverslip. A TCS SP8 epifluorescence confocal microscope (Leica microsystems, Wetzlar, Germany) connected to Leica LAS AF 3 software was used to investigate the surface structure, the distribution of Fe nanoparticles (Fe-NP), and the adsorption of albumin on alginate and alginate-fibrin hydrogels (Figure 1C). Surface structures were detected in the bright field mode when selecting the transmittance light detector mode and light entering the photomultiplier tube has been transmitted. To detect the Fe-NP, the excitation wavelength was at 470 nm while the emission wavelength was in the range of 478–528 nm. Adsorption of TRITC-coupled albumin on the gels was studied with an excitation wavelength at 555 nm, while the emission wavelength was in the range of 563–620 nm. All obtained confocal microscopy images were processed with ImageJ software (ImageJ, Maryland, USA).

### 2.5. Cell Culture

For cell seeding, unmodified and modified alginate hydrogels were separated from the base-layer of agarose/CaCl$_2$ and transferred into new tissue culture plates. Human umbilical cord vein endothelial cells (HUVEC) (Pelobiotech, Planegg, Germany) of passage two to seven were cultured in EBM-2 medium (Lonza, Köln, Germany) and seeded to the hydrogels in 96-well-plates (7500 HUVEC in 200 µL medium) or in 24-well-plates (47100 HUVEC in 500 µL medium). Medium was changed after 48 h.
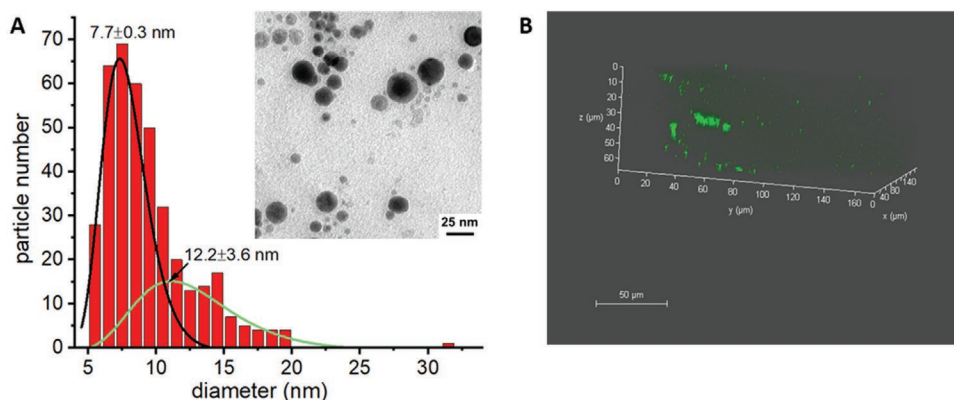
**Figure 2.** A) Particle size distributions and representative TEM images of Fe nanoparticles generated by the laser ablation of Fe metal plate in alginate aqueous solutions. B) Laser scanning microscopy 3D images of gelated alginate filled with Fe nanoparticles.

## 2.6. Viability Assay

To quantify the viability of HUVEC on the different hydrogels a WST-8-assay (Colorimetric Cell Viability Kit (PromoCell, Heidelberg, Germany)) was performed after 72 h in 96-well-plates ($n = 6$ for each group). Cell culture medium was reduced to 100 µL, 10 µL dye was added, and the well-plates were incubated at 37 °C and 5% $CO_2$ for 2 h. 100 µL of the supernatant was then transferred to a microtest plate and absorption at 450 nm was measured at a microtiter plate reader. Statistical calculations were performed by GraphPad Prism 5 (GraphPad Software, San Diego, California). The mean and standard deviation or standard error of the mean was calculated for all values obtained as indicated. Multiple comparisons between groups were performed by one-way ANOVA and Sidak´s post test. Differences were considered significant at $p < 0.05$. Significance levels were given as follows: * $p < 0.05$ and ** $p < 0.01$.

## 2.7. Live/Dead Staining

Live/dead staining was performed after 72 h in 24-well-plates ($n = 2$ for each group). For this, cell culture medium was removed and the hydrogels were washed twice with PBS. Hydrogels were incubated with 300 µL calcein/ethidium-homodimer solution (Life Technologies, Darmstadt, Germany) for 45 min under light protection. After the staining solution was removed, hydrogels were washed with PBS as before. Hydrogels were transferred to object slides and viability and morphology were evaluated by fluorescence microscopy imaging live cells green (calcein) and dead cells red (ethidium-homodimer) (Figure 1D). Graphical editing was conducted with ImageJ software.

## 3. Results

### 3.1. Characterization of Laser-Generated Iron-Alginate Solution, Cross-linked Hydrogel Surfaces and Rheological Properties

We characterized the laser synthesized Fe-NPs in alginate solutions with TEM and the results showed spherical Fe-NPs

and size distributions best fitted with two log-normal fits with two mean diameters, one at 7.7 ± 0.3 nm and the other at 12.2 ± 3.6 nm (**Figure 2**A). Meanwhile, the FeNPs distribution in the cross-linked alginate matrix was observed with LSM (Figure 2B). The results showed that most nanoparticles were homogeneously distributed in alginate, however, slight particle agglomeration was also found.

Pure alginate gel and alginate with 10 mg mL$^{-1}$ fibrin with or without embedded Fe-NP (200 µg mL$^{-1}$) were analyzed for their wettability. **Figure 3**A shows the air bubble droplets in water on each surface and the respective contact angles. The relatively low contact angle of pure alginate was significantly increased by fibrin-blending (1.9-fold for 10 mg mL$^{-1}$ fibrin, $p < 0.01$) indicating an increasing hydrophobicity of the blended hydrogel (Figure 3B). Fe-NP, in contrast, had the opposite effect since they decreased the contact angle in all hydrogels to the same extent (0.4-fold, significant for fibrin-blended gels with $p > 0.01$ [5 mg mL$^{-1}$] and $p < 0.05$ [10 mg mL$^{-1}$] for both Fe-NP concentrations). A similar effect was observed with respect to the roughness measured by AFM showing an increased roughness of alginate gels blended with fibrin which was decreased by the incorporation of Fe-NP in both types of gel (Figure S1, Supporting Information). Roughness parameters given in Table S1, Supporting Information, indicate a 1.2- and 1.4-fold increase for the mean roughness, $R_a$, and the root mean square roughness, $R_q$, by fibrin-blending, respectively. This was also reflected by the maximum peak to valley high, which was 1.82-fold increased by fibrin-blending of alginate and reduced to the same level by Fe-NP incorporation for both types of gels. Rheological characterization indicated both an increased storage and elastic modulus (1.9-fold, $p > 0.05$) by the incorporation of 200 µg mL$^{-1}$ Fe-NP in pure alginate gels which was reversed by the blending with fibrin to baseline levels. Incorporation of 100 µg mL$^{-1}$ Fe-NP did not exert the same effect (Figure 3C,D). Taken together, alginate modification with fibrin resulted in more hydrophobic and less stiff gels whereas Fe-NP partially reversed these effects, which may indicate an interaction between nanoparticles and fibrin fibers.

This was confirmed by a surface characterization by LSM. Alginate hydrogels were smooth and had no observable surface textures, while Fe-NP distributed randomly within the
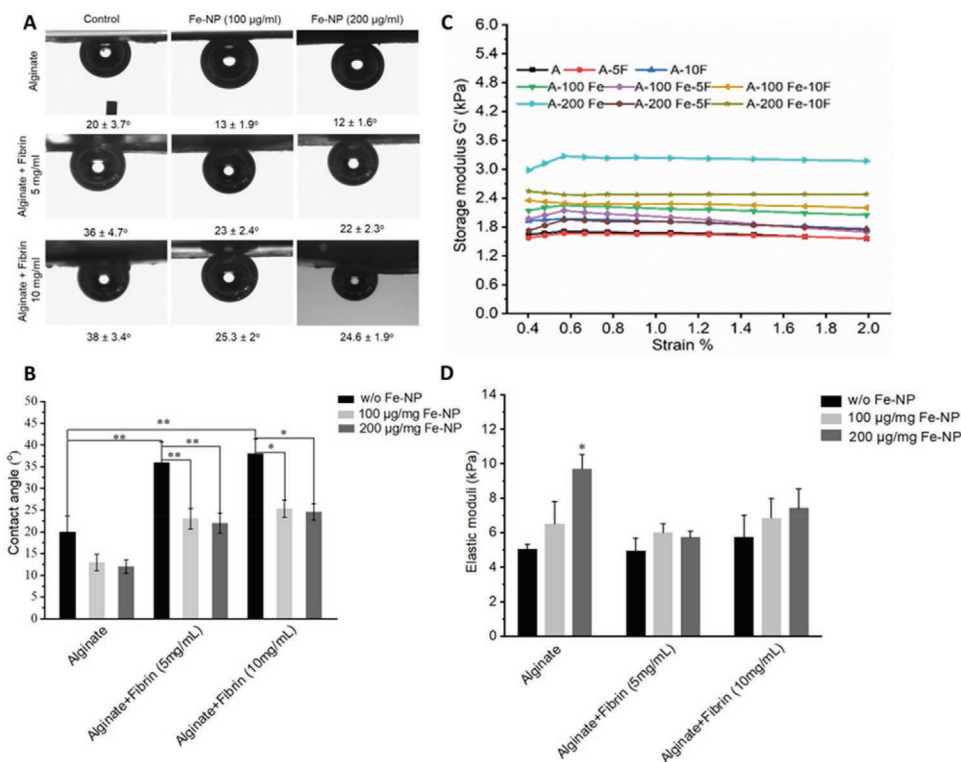
**ADVANCED
SCIENCE NEWS**

www.advancedsciencenews.com

**ADVANCED
MATERIALS
INTERFACES**

www.advmatinterfaces.de

**Figure 3.** Surface characterization of alginate hydrogels. A) Contact angles (CA) of air bubble droplets in the water on the surface of biomaterials at room temperature. B) Bar diagram of averaged contact angles. C) Storage modulus G′ measured over a decade of oscillation strain in the range of 0.4–2% and D) representative elastic modulus E calculated from G′ at 1% strain. Shown are mean ± SD of three independent experiments analyzed by one-way-ANOVA and Tukey post test. $*p \leq 0.05$ and $**p \leq 0.01$. A = Alginate, 100/200Fe = 100/200 µg mL$^{-1}$ iron nanoparticles, 5/10F = 5/10 mg mL$^{-1}$ fibrin.

gel (**Figure 4**A). Fibrin-blended gels, on the other hand, have rougher surfaces with clearly visible fibrin fibers. Interestingly, Fe-NPs were observed to accumulate along with these fibers

(Figure 4B) and controls (Figure S3, Supporting Information) clearly show that the detected signals did not originate from autofluorescence of the matrix.
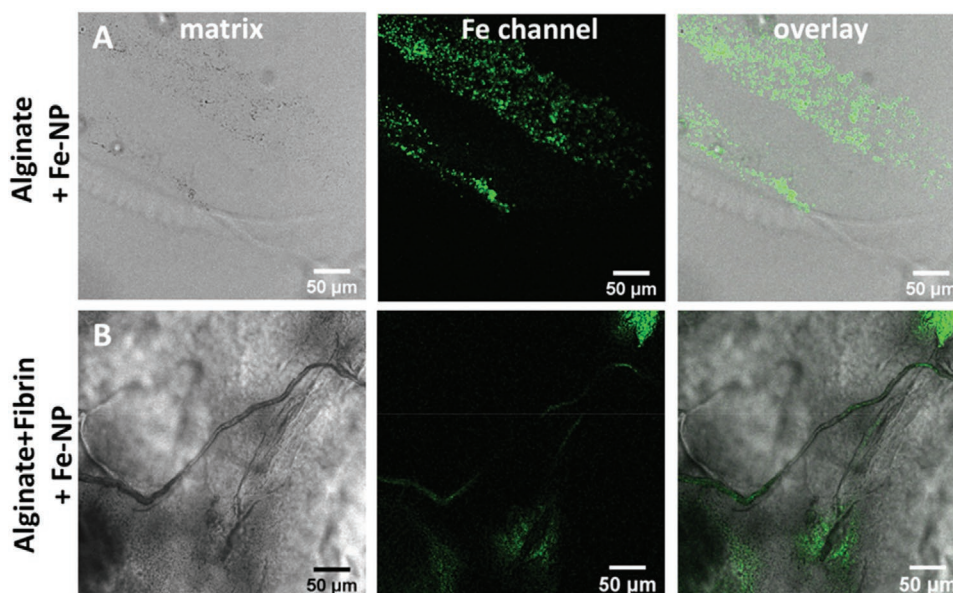


**Figure 4.** Surface characterization of alginate based hydrogels by confocal laser scanning microscopy A) enriched with 200 µg mL$^{-1}$ Fe-NPs and B) additional blending with 10 mg mL$^{-1}$ fibrin showing the matrix structure (left), Fe-NP scattering at the wavelength of 488 nm (middle), and the overlay of both channels (right).
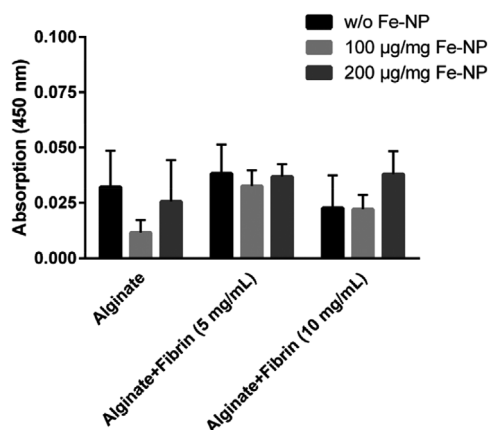
**ADVANCED**
**SCIENCE NEWS**
www.advancedsciencenews.com

**ADVANCED**
**MATERIALS**
INTERFACES
www.advmatinterfaces.de

**Figure 5.** Endothelial cell viability on alginate hydrogels blended with 5 or 10 mg mL$^{-1}$ fibrin and enriched with 100 or 200 µg mL$^{-1}$ iron nanoparticles (Fe-NP) assessed by WST-8 assay. Shown are means ± SEM of three independent experiments measured in duplicate and analyzed by 1-way ANOVA and Sidak's post test. No significant differences were calculated.

### 3.2. Effect of Iron Nanoparticles and Fibrin on Endothelial Cell Seeding

To evaluate the impact of these material properties on living cells, endothelial cell viability after seeding them onto alginate hydrogels with or without embedded Fe-NPs in concentrations of 100 and 200 µg mL$^{-1}$ was assessed after 72 h by WST-8-assays. Only low absorption at a wavelength of 450 nm could be measured on either alginate hydrogel (**Figure 5**), which indicates a low overall viability.

Live/dead staining showed extremely few cells with rounded morphology on pure alginate gels and a slightly increased number of cells with an occasionally more physiological shape on the Fe-NP embedded gels (**Figure 6**A–C). Nevertheless, high numbers of dead cells indicate insufficient biocompatibility. The blending of alginate hydrogels with fibrin in both concentrations and in combination with Fe-NP did not result in higher absorption in the viability assay (Figure 5). Interestingly, live–dead staining revealed a physiological spindle-like shape of all cells of which the majority survived (Figure 6D–I); however, global viability was not enhanced.

Overall, the upgrading of alginate hydrogels by either Fe-NP or fibrin did not have a toxic effect on endothelial cell viability but also did not enhance biocompatibility significantly. Only the addition of fibrin seems to have a beneficial effect on endothelial cell adhesion and morphology in live–dead staining; nevertheless, a significant effect on cell viability could not be achieved.

Storage of hydrogels could induce the formation of degenerative pores that may improve cell attachment and thereby increase viability. However, storage in distilled water of all types of gel for 8 days did not change the viability of seeded endothelial cell markedly (Figure S2, Supporting Information).

### 3.3. Effect of Serum Protein Coating

To test a putative beneficial effect of serum proteins, gels were coated with FBS for 3 h prior to endothelial cell seeding and assessed as before. WST-8-assays showed that the poor viability of endothelial cell seeded on pure alginate gels with or without
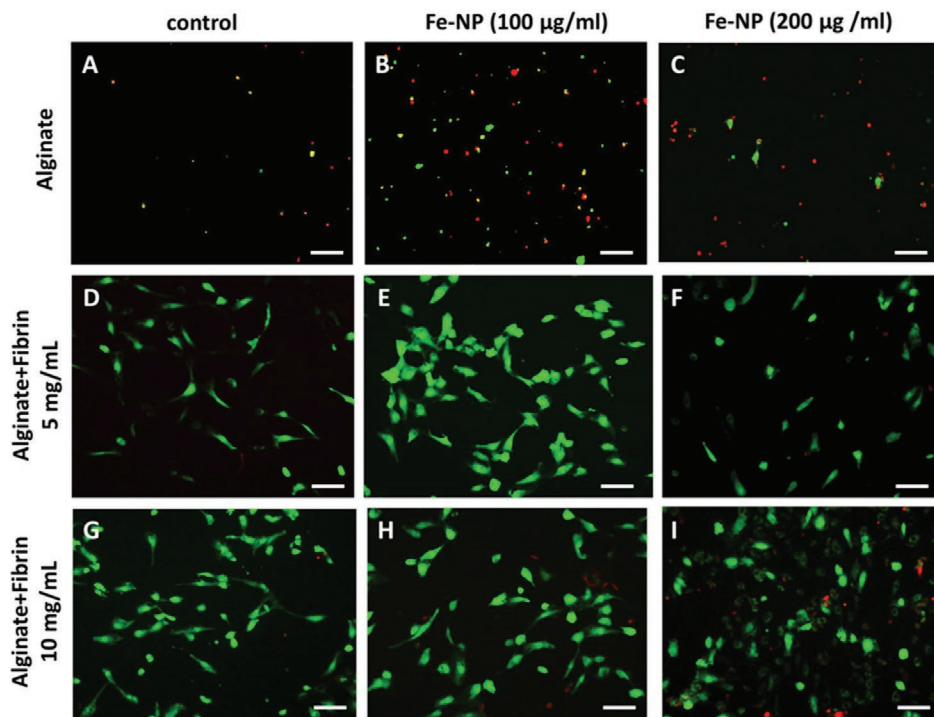


**Figure 6.** Endothelial proliferation and morphology on A–C) pure alginate hydrogels blended with D–F) 5 mg mL$^{-1}$ fibrin or G–I) 10 mg mL$^{-1}$ fibrin and enriched with 100 µg mL$^{-1}$ Fe-NPs (middle) or 200 µg mL$^{-1}$ Fe-NP (right) assessed by live-dead staining. Shown are typical images of two independently stained gels. Scale bar 100 µm.
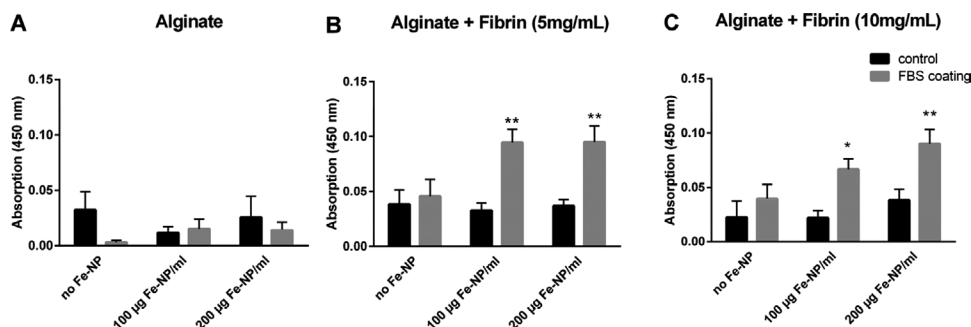
**ADVANCED
SCIENCE NEWS**
www.advancedsciencenews.com

**ADVANCED
MATERIALS
INTERFACES**
www.advmatinterfaces.de

**Figure 7.** Effect of FBS coating on endothelial cell viability on A) pure alginate hydrogels blended with B) 5 mg mL$^{-1}$ fibrin or C) 10 mg mL$^{-1}$ fibrin and enriched with 100 or 200 µg mL$^{-1}$ Fe-NPs assessed by WST-8 assay. Shown are means ± SEM of three independent experiments measured in duplicate and analyzed by 1-way ANOVA and Sidak's post test. *$p \leq 0.05$ and **$p \leq 0.01$ vs control.

Fe-NP was not improved by FBS coating (**Figure 7**A). Also, in alginate-fibrin gels without Fe-NP, FBS coating did not result in a significant increase in absorption. In contrast, the combination of fibrin plus Fe-NP in both concentrations resulted in a significant 2.9- and 2.6-fold increase for 5 mg mL$^{-1}$ fibrin ($p < 0.01$) and in a 3.0- and 2.4-fold increase for 10 mg mL$^{-1}$ fibrin ($p < 0.05$ and $<0.01$; Figure 7B,C).

Live/dead staining of the respective groups confirmed the supportive effect of FBS coating on alginate-fibrin gels enriched with Fe-NP (**Figure 8**). The combination of all three components resulted in an almost confluent endothelial layer with physiological cell morphology (Figure 8G,H,K,L). The effect was most obvious for the 10 mg mL$^{-1}$ fibrin blending enriched with 200 µg mL$^{-1}$ Fe-NP (Figure 8L) suggesting a concentration-dependent influence of fibrin and Fe-NP in combination with serum proteins.

LSM confirmed this synergistic effect of fibrin, Fe-NP, and serum proteins by visualizing the adsorption of TRIC-coupled albumin on the various surfaces. Whereas pure alginate and fibrin-blended alginate hydrogels only showed faint and dif-

fused protein agglomerates (Figure S3, Supporting Information); the fibrin-alginate gels enriched with Fe-NP showed an agglomerated albumin deposition that colocalized with Fe-NP along the fibrin fibers (**Figure 9**).

In summary, we showed that fibrin-blended alginate hydrogels enriched with Fe-NPs and coated with serum proteins are a suitable biomaterial to promote strong endothelialization, while the synergistic recombination of the three modifications I) fibrin blending, II) Fe-NP, and III) serum proteins is a mandatory requirement to achieve these effects.

## 4. Discussion

### 4.1. Alginate Gels

Alginate consists of $\alpha$-L-guluronic acid and $\beta$-D-mannuronic-acid, forming G- and M-blocks and gelated to a polymer by binding divalent cations between the G-blocks of different alginate chains. The high number of negative charges and a
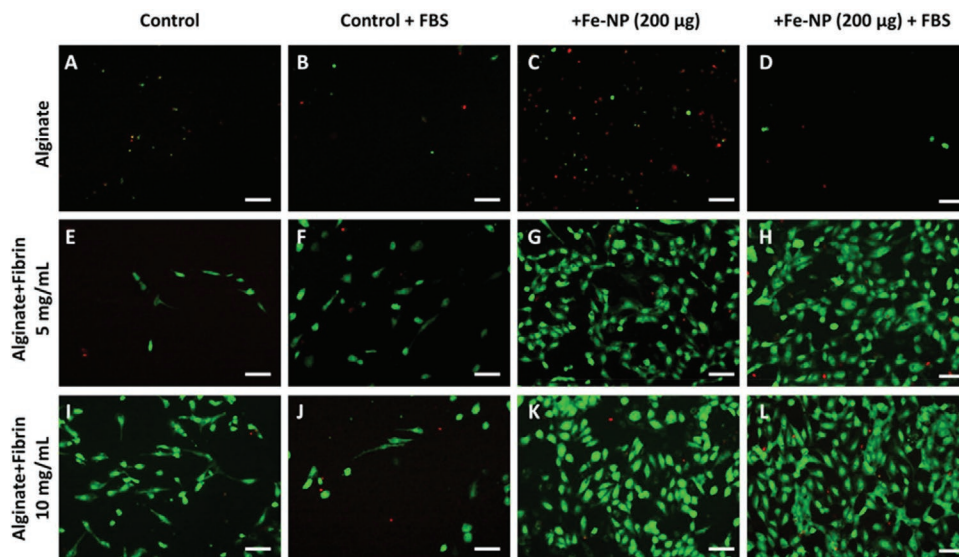


**Figure 8.** Effect of FBS coating on endothelial proliferation and morphology on A–D) pure alginate hydrogels blended with E–H) 5 mg mL$^{-1}$ fibrin or I–L) 10 mg mL$^{-1}$ fibrin and enriched with 200 µg mL$^{-1}$ Fe-NPs assessed by live-dead staining. Shown are typical images of two independently stained gels. Scale bar 100 µm.
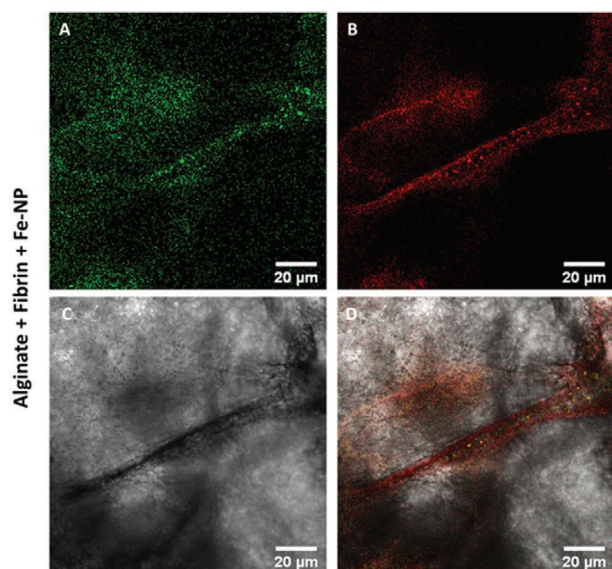
**ADVANCED**
**SCIENCE NEWS**
www.advancedsciencenews.com

**ADVANCED**
**MATERIALS**
**INTERFACES**
www.advmatinterfaces.de

**Figure 9.** Serum protein deposition on alginate hydrogels. Confocal microscopy images of alginate hydrogels blended with 10 mg mL$^{-1}$ fibrin and enriched with 200 mg mL$^{-1}$ iron nanoparticles (Fe-NP) after incubation with TRITC fluorophore-labeled albumin in FBS solution: A) detected Fe-NP at 488 nm, B) detected albumin at 555 nm, C) matrix and D) overlay picture.

pronounced surface wettability plus the absence of any cellular adhesion structures is the molecular basis for the high hydrophilicity observed in this study leading to the non-fouling effect that broadly prevents cellular attachment.[8,11] In this study, the non-fouling effect became apparent on alginate-hydrogels resulting in a high rate of dead HUVEC in live/dead staining and low viability in WST-8-assays. As cellular adhesion is the initial mechanism in the interaction between cells and substrate surfaces, it is essential for subsequent proliferation to a confluent cell layer and impeded cell adhesion therefore accounts for "Anoikis" (homelessness)-induced apoptosis.[23]

### 4.2. Effect of Iron Nanoparticles

Fe-NPs distributed incidentally throughout the alginate hydrogel matrix (Figure 2B) are enhancing hydrogel stiffness (Figure 3C). Furthermore, wettability measurements showed increased hydrophilicity (Figure 3A,B) whereas surface roughness decreased (Figure S1, Supporting Information). Overall, there was no effect on endothelial cell adhesion and viability (Figures 5 and 6) indicating that Fe-NPs as the only additive in alginate (in contrary to their combination with serum proteins, compare Section 4.4) are insufficient to reduce non-fouling effects of alginate hydrogels for enhanced biocompatible properties.

Metal ions exert several effects on the properties of alginate hydrogels related to cell adhesion and proliferation. On the one hand, cross-linking with $Ca^{2+}$, $Mg^{2+}$, and $Sr^{2+}$ ions has been shown to increase the mechanical strength of alginate gels[12] which could positively affect cellular adhesion and migration, an effect called durotaxis,[24] which also was confirmed in this study. On the other hand, cross-linking with ferric, barium, and aluminum ions substantially decreased the high wettability

of alginate surfaces[13] among which ferric ions also promoted adsorption of serum proteins such as vitronectin. These effects accounted for an improved attachment and proliferation of humane dermal fibroblasts, a rather robust and fast proliferating cell type, also used in cytocompatibility tests postulated in the test conditions of DIN EN:ISO 10993.[25] The incorporation of Fe-NP as a source for sustained ferric ion release was able to promote cellular compatibility as well as cellular adhesion also for endothelial cells displaying a lower proliferative potential but confirming biocompatibility of alginate hydrogels with Fe-NPs.[15] Interestingly, in our study none of these effects became obvious. Fe-NP increased wettability (Figure 3A,B) which may have caused the poor attachment and limited survival of endothelial cells on alginate gels filled with Fe-NP (Figures 5 and 6A–C). Another reason why the potential benign effects of iron were not observed in this study may be attributed to ion release and associated gel cross-linking. In the alginate-based hydrogel cross-linking process, the basal $Ca^{2+}$ concentration was enough to complete the gelation. Subsequently alginate and the obtained hydrogel patches were washed with PBS and water, thus extra $Ca^{2+}$ could be removed. Nonetheless, it is known from our previous studies that the release of Fe ions from laser-fabricated Fe-NPs embedded in alginate tends to follow complex kinetics not solely driven by diffusion and iron oxidation but strongly affected by oxide solubility and especially potential interactions between iron ions and the alginate matrix.[16] The latter effect, caused by a stronger affinity of heavy metal ions to alginate, in contrast to $Ca^{2+}$,[26] would induce an ion exchange and may be responsible for trapping some amounts of the released iron in the gel matrix. Furthermore, the additional amount of iron ions could intensify the gelation process, leading to a more dense hydrogel network which also impedes ion release rates, as observed in our previous studies at high iron mass loads.[16] Consequently, trapping of iron ions in a more dense gel matrix may be why the biological effect of the iron ions is less than anticipated and the Fe-NPs alone have no observable effect on the cells. Since Fe-NP were fabricated by identical procedures and LSM showed a scattered distribution of the nanoparticles in alginate gels (Figure 4A), this difference could also be due to the alginate´s natural origin and presumably variable ratios between G- and M-blocks. Indeed, it has been shown that G-blocks rather than M-blocks account for the proliferative effect of ferric ions on fibroblasts.[27] A higher amount of G-blocks is also associated with a more porous structure and hence a higher diffusion capacity for proteins.[28]

### 4.3. Effect of Fibrin in Alginate Hydrogels

The enrichment of alginate hydrogels with fibrin resulted in a decreased wettability (Figure 3A,B) and a highly roughened surface (Figure S1, Supporting Information). Rheological studies revealed a lower stiffness of fibrin-enriched hydrogels (Figure 3C,D). Despite significantly altered surface characteristics, the effect on endothelial cell viability was limited. Alginate-fibrin composites showed isolated endothelial cells with elongated morphology and a reduced number of dead cells, nevertheless, a homogenous endothelialization was not induced (Figure 6).

Alginate biofunctionalized with RGD peptides as adhesive sequences is known to enhance cellular adhesion and proliferation.[11] Fibrin exposes RGD peptides[29] favoring integrin clustering and formation of focal adhesions[30,31] and therefore served as an adhesive molecule in the inherent alginate structure by promoting endothelial cell adhesion, proliferation, and migration via integrin receptor $\alpha v \beta 3$. This effect was visible by live/dead staining depicting a reduced amount of dead endothelial cells and a physiological spindle-like morphology of living cells (Figure 6). Besides this biochemical effect, also a topographical effect of fibrin fibers is imaginable, since LSM revealed a considerably rougher surface structure with single visible fibers in alginate-fibrin hydrogels (Figure 4B). AFM showed that fibrin clearly increased roughness parameters of alginate gels (Figure S1, Supporting Information). Moreover, the observed reduced wettability of alginate-fibrin gels may have contributed to this effect (Figure 3A,B). Less hydrophilic surfaces enable the development of dehydration forces being essential for protein binding.[32] However, since colorimetric assay did not show enhanced viability (Figure 5), the effect of fibrin on endothelial cell adhesion appears to be limited to focal fibrin fibers and does not affect the whole surface structure.

### 4.4. Synergistic Effect of Iron Nanoparticles and Fibrin on Alginate Hydrogels via Protein Absorption

Visualization of Fe-NP in fibrin-blended alginates showed Fe-NP agglomerating along the fibrin fibers (Figure 4B). Therefore, a direct interaction between Fe-NPs and fibrin can be supposed. In physiological environments, nanoparticles have been shown to build a protein corona.[33] Interestingly, in our study Fe-NPs assembled on fibrin fibers also seemed to attract serum albumin since LSM clearly showed that albumin deposition followed the structure of Fe-NP-covered fibrin fibers (Figure 9) whereas alginate gels containing only fibrin showed merely diffused protein agglomeration (Figure S3, Supporting Information). Thus, both alginate modifications together with SPC synergize most likely to an adhesive triple complex for endothelial cell adhesion, promoting proliferation, and viability. Besides, local adhesive complexes, fibrin plus Fe-NP incorporation result in a surface root mean square roughness of 32 nm which is known to highly support fibronectin adsorption[34] (Figure S1, Supporting Information). Protein adsorption is the first process in the interaction between cells and a given surface and thus its quantitative and qualitative protein adsorption capacity determines essentially its biocompatibility.[35] The primary interaction between cells and adhesion proteins occurs via integrins being activated by the exposed binding sequences. Integrins are transmembrane receptors to transduce surface characteristics represented by the adsorbed protein profile into basal cellular responses comprising cellular adhesion, morphology, motility, and proliferation.[36] The absence of integrin activation results in cellular apoptosis[23] emphasizing the significance of adequate protein adsorption and following integrin activation. Since increasing protein concentrations in solution are known to accelerate surface protein adsorption,[32] the effect of SPC on cellular adhesion seems to be consequential. Though serum proteins were present in lower concentrations in all cell

culture experiments (EBM-2 medium contains 2% FBS), obviously a higher concentration was necessary to achieve this effect. Extrapolating our result to a clinical scenario, alginate modified by fibrin and Fe-NP will encounter sufficiently high serum albumin concentrations after implantation by the bloodstream and thus will provide a promising surface for rapid and stable endothelialization. A closed endothelialization is the best means to avoid thrombo-embolic events which is one purpose of the non-fouling effect. Whether this biomaterial also displays a surface which in parallel impairs biofilm formation will have to be the subject of further studies.

### 4.5. Hemocompatibility of Alginate-Fibrin Hydrogels Enriched with Iron Nanoparticles

A limitation of this study is the missing hemocompatibility testing. Hemocompatibility is an important topic which has to be profoundly analyzed according to ISO standard.[37] Nevertheless, at this early preclinical stage a hypothesis about the hemocompatibility of the composite hydrogel can be made on the basis of the particular components and has to be evaluated in further research projects including hemolysis, cell counts, and the activation of platelets, leukocytes, and coagulation.

Alginic acid as basis material is characterized by a "nonfouling" property preventing not only protein adsorption but also platelet adhesion.[9] This is a crucial feature of stent surface materials since in-stent thrombosis is a dreaded complication in stent-therapy.[38] By implementation of the dual antiplatelet therapy (DAPT) the incidence of acute in-stent thrombosis caused by the presence of the stent material significantly decreased.[39,40] Late in-stent thrombosis due to incomplete endothelialization[41] remains a major problem so that research on new stent materials mainly focuses on promoting complete endothelialization of the stent surface.[42] Since alginate hydrogels impede endothelial cell adhesion, we upgraded the alginate matrix with the natural polymer fibrin being known for its various adhesion sites for endothelial cells[18] and its high biocompatibility as a stent coating material[4,6] or vascular graft.[18,43] Furthermore, Fe-NPs have been shown to reinforce the fibrin matrix and to enhance endothelial cell proliferation.[13,15,44]

On the whole, we hypothesize based on available literature that Fe-NP enriched alginate-fibrin hydrogels synergize their individual antithrombotic properties to a compound highly hemocompatible stent coating material. While alginic acid prevents acute in-stent thrombosis due to direct inhibition of platelet adhesion, fibrin and Fe-NPs enables complete endothelialization and therefore ensure long-term antithrombotic effects.

## 5. Conclusion

In summary, we demonstrated the role of Fe-NP and fibrin in the modification of alginate and effects on their wettability, surface roughness, and elastic modulus. This, in turn, led to a promoted serum protein absorption and thereby contributed to a confluent endothelialization by enhancing cellular adhesion, proliferation, and viability, and thus displays a promising stent

coating biomaterial. This stent coating biomaterial benefits from synergistic effect of fibrin, Fe-NPs, and serum proteins. To further evaluate its applicability, alginate-fibrin stability, nanoparticle elution, hemocompatibility, and the effect on bacterial adhesion will have to be analyzed, both as the base material as well as after its coating on stent surfaces.

## Supporting Information

Supporting Information is available from the Wiley Online Library or from the author.

## Acknowledgements

## Conflict of Interest

The authors declare no conflict of interest.

## Data Availability Statement

Research data are not shared.

## Keywords

[1] F. Otsuka, R. A. Byrne, K. Yahagi, H. Mori, E. Ladich, D. R. Fowler, R. Kutys, E. Xhepa, A. Kastrati, R. Virmani, M. Joner, *Eur. Heart J.* **2015**, *36*, 2147.

[2] S. Pursnani, F. Korley, R. Gopaul, P. Kanade, N. Chandra, R. E. Shaw, S. Bangalore, *Circ.: Cardiovasc. Interventions* **2012**, *5*, 476.

[3] R. A. Byrne, M. Joner, A. Kastrati, *Eur. Heart J.* **2015**, *36*, 3320.

[4] S. H. Im, Y. Jung, S. H. Kim, *Acta Biomater.* **2017**, *60*, 3.

[5] J. Chu, L. Chen, Z. Mo, G. L. Bowlin, B. A. Minden-Birkenmaier, Y. Morsi, A. Aldalbahi, M. El-Newehy, W. Wang, X. Mo, *Acta Biomater.* **2020**, *111*, 102.

[6] S. Weinandy, L. Rongen, F. Schreiber, C. Cornelissen, T. C. Flanagan, A. Mahnken, T. Gries, T. Schmitz-Rode, S. Jockenhoevel, *Tissue Eng., Part A* **2012**, *18*, 1818.

[7] M. Liu, X. Yue, Z. Dai, L. Xing, F. Ma, N. Ren, *Langmuir* **2007**, *23*, 9378.

[8] M. Morra, C. Cassineli, *J. Biomater. Sci., Polym. Ed.* **1999**, *10*, 1107.

[9] J. F. Keuren, S. J. Wielders, G. M. Willems, M. Morra, L. Cahalan, P. Cahalan, T. Lindhout, *Biomaterials* **2003**, *24*, 1917.

[10] G. A. Junter, P. Thebault, L. Lebrun, *Acta Biomater.* **2016**, *30*, 13.

[11] J. A. Rowley, G. Madlambayan, D. J. Mooney, *Biomaterials* **1999**, *20*, 45.

[12] G. Kaklamani, D. Cheneler, L. M. Grover, M. J. Adams, J. Bowen, *J. Mech. Behav. Biomed. Mater.* **2014**, *36*, 135.

[13] I. Machida-Sano, M. Hirakawa, H. Matsumoto, M. Kamada, S. Ogawa, N. Satoh, H. Namiki, *Biomed. Mater.* **2014**, *9*, 025007.

[14] K. Brändle, T. C. Bergmann, A. Raic, Y. Li, N. Million, C. Rehbock, S. Barcikowski, C. Lee-Thedieck, *ACS Appl. Bio Mater.* **2020**, *3*, 4766.

[15] A. Blaeser, N. Million, D. F. D. Campos, L. Gamrad, M. Köpf, C. Rehbock, M. Nachev, B. Sures, S. Barcikowski, H. Fischer, *Nano Res.* **2016**, *9*, 3407.

[16] Y. Li, C. Rehbock, M. Nachev, J. Stamm, B. Sures, A. Blaeser, S. Barcikowski, *Nanotechnology* **2020**, *31*, 405703.

[17] R. M. Visalakshan, M. N. MacGregor, S. Sasidharan, A. Ghazaryan, A. M. Mierczynska-Vasilev, S. Morsbach, V. Mailänder, K. Landfester, J. D. Hayball, K. Vasilev, *ACS Appl. Mater. Interfaces* **2019**, *11*, 27615.

[18] F. M. Shaikh, A. Callanan, E. G. Kavanagh, P. E. Burke, P. A. Grace, T. M. McGloughlin, *Cells Tissues Organs* **2008**, *188*, 333.

[19] C. E. Vorwald, T. Gonzalez-Fernandez, S. Joshee, P. Sikorski, J. K. Leach, *Acta Biomater.* **2020**, *108*, 142.

[20] D. Zhang, B. Gökce, S. Barcikowski, *Chem. Rev.* **2017**, *117*, 3990.

[21] S. Lau, D. Eicke, M. C. Oliveira, B. Wiegmann, C. Schrimpf, A. Haverich, R. Blascyk, M. Wilhelmi, C. Figueiredo, U. Boeer, *Tissue Eng., Part A* **2018**, *24*, 432.

[22] T. R. Cox, C. D. Madsen, *Bio-Protoc.* **2017**, *7*, e2101.

[23] S. M. Frisch, H. Francis, *J. Cell Biol.* **1994**, *124*, 619.

[24] C. M. Lo, H. B. Wang, M. Dembo, Y. L. Wang, *Biophys. J.* **2000**, *79*, 144.

[25] I. Machida-Sano, Y. Matsuda, H. Namiki, *Biomed. Mater.* **2009**, *4*, 025008.

[26] Y. Jodra, F. Mijangos, *Water Sci. Technol.* **2001**, *43*, 237.

[27] I. Machida-Sano, S. Ogawa, H. Ueda, Y. Kimura, N. Satoh, H. Namiki, *Int. J. Biomater.* **2012**, *2012*, 820513.

[28] A. Martinsen, G. Skjåk-Bræk, O. Smidsrød, *Biotechnol. Bioeng.* **1989**, *33*, 79.

[29] A. Henschen, *Thromb. Res.* **1983**, *29*, 27.

[30] S. Yakovlev, I. Mikhailenko, G. Tsurupa, A. M. Belkin, L. Medved, *Thromb. Haemostasis* **2014**, *112*, 1244.

[31] A. M. Belkin, G. Tsurupa, E. Zemskov, Y. Veklich, J. W. Weisel, L. Medved, *Blood* **2005**, *105*, 3561.

[32] M. Holmberg, X. Hou, *Langmuir* **2009**, *25*, 2081.

[33] T. Cedervall, I. Lynch, S. Lindman, T. Berggard, E. Thulin, H. Nilsson, K. A. Dawson, S. Linse, *Proc. Natl. Acad. Sci. U. S. A.* **2007**, *104*, 2050.

[34] K. Rechendorff, M. B. Hovgaard, M. Foss, V. P. Zhdanov, F. Besenbacher, *Langmuir* **2006**, *22*, 10885.

[35] C. J. Wilson, R. E. Clegg, D. I. Leavesley, M. J. Pearcy, *Tissue Eng.* **2005**, *11*, 1.

[36] J. D. Humphries, M. R. Chastney, J. A. Askari, M. J. Humphries, *Curr. Opin. Cell Biol.* **2019**, *56*, 14.

[37] M. Weber, H. Steinle, S. Golombek, L. Hann, C. Schlensak, H. P. Wendel, M. Avci-Adali, *Front. Bioeng. Biotechnol.* **2018**, *6*, 99.

[38] I. Iakovou, T. Schmidt, E. Bonizzoni, L. Ge, G. M. Sangiorgi, G. Stankovic, F. Airoldi, A. Chieffo, M. Montorfano, M. Carlino, L. Michev, N. Corvaja, C. Brigurio, U. Gerckens, E. Grube, A. Colombo, *JAMA, J. Am. Med. Assoc.* **2005**, *293*, 2126.

[39] F. Alfonso, A. Suarez, D. J. Angiolillo, M. Sabate, J. Escaned, R. Moreno, R. Hernández, C. Banuelos, C. Macaya, *Heart* **2004**, *90*, 1455.

[40] M. E. Bertrand, H. J. Rupprecht, P. Urban, A. H. Gershlick, F. T. C. Investigators, *Circulation* **2000**, *102*, 624.

[41] A. V. Finn, M. Joner, G. Nakazawa, F. Kolodgie, J. Newell, M. C. John, H. K. Gold, R. Virmani, *Circulation* **2007**, *115*, 2435.

[42] K. Zhang, T. Liu, J. A. Li, J. Y. Chen, J. Wang, N. Huang, *J. Biomed. Mater. Res., Part A* **2014**, *102*, 588.

[43] O. Kaplan, T. Hierlemann, S. Krajewski, J. Kurz, M. Nevoralová, M. Houska, T. Riedel, Z. Riedelová, J. Zárubová, H. P. Wendel, E. Brynda, *J. Biomed. Mater. Res., Part A* **2017**, *105*, 2995.

[44] M. N. Kirichenko, L. L. Chaikov, S. V. Krivokhizha, A. S. Kirichenko, N. A. Bulychev, M. A. Kazaryan, *J. Chem. Phys.* **2019**, *150*, 155103.